Taylor & Francis
Taylor & Francis Group

Energy performance of water strip modules for industrial heating in real operation conditions: Steady-state and CFD analyses

Marco Noro, Simone Mancin & Michele Calati |

Published online: 25 Jul 2023.

Submit your article to this journal

View related articles

Taylor & Francis
Taylor & Francis Group

ENVIRONMENTAL MANAGEMENT & CONSERVATION | RESEARCH ARTICLE

🔓 OPEN ACCESS   ✔ Check for updates

Energy performance of water strip modules for industrial heating in real operation conditions: Steady-state and CFD analyses

Marco Noro[a], Simone Mancin[a] and Michele Calati[a]

[a]Department of Management and Engineering, University of Padua, Vicenza, Italy

ABSTRACT
The objective of this study is the theoretical evaluation of the energy performance of a radiant strips heating system fed with hot water by varying the operating conditions. First, the convective coefficients and the heating power (both convective and radiant parts) of the heating system are evaluated in steady-state conditions by simulating heat exchange similar to real operating conditions (such as the presence of a ventilation system, the opening of doors, windows, or skylights, etc.), in comparison with the nominal data. To carry out this preliminary assessment, different references in the scientific literature are considered with respect to experimental measurements and numerical simulations for similar applications. The steady-state analysis revealed that the increase in the overall yield of the heating strips, compared to the data measured according to the EN 14,037 standard, is in the order of 30%. Afterward, a CFD analysis is reported to dynamically study the effect of the above-mentioned typical situations of real operation of the system in industrial sheds. The CFD analysis confirms that the presence of constant air exchange leads to an improvement of more than 30% in the performance of the water strip system. The main conclusion is that designing the water strip system following the EN 14,037 standard probably will oversize the industrial heating plant.

1 Introduction

Usually, Heating, Ventilation and Air Conditioning (HVAC) systems are dimensioned based on static design values and so they are oversized during most of the operation time. For this reason, Vogt et al., (2022) compared the performance of four main control schemes in a battery production site. They found that even simple control approaches, without any predictions, have a good energy saving potential of up to 20.2% compared to the initial state. Recently, an energy efficiency assessment tool for industrial environment at the three main organizational levels (plant, process, and machine) was developed based on a literature review (Richter et al., 2023). Both micro and macro-scale impacts of implementing energy-efficient HVAC systems were analyzed in (Shook et al., 2023) by means of a useful integration of the industrial building energy data with the macroeconomic regional economic flow model.

Industrial facilities were studied in the case of energy retrofit (Trianni et al., 2014), focusing both on the thermal envelope (Katunska et al., 2014) and on technical building services, such as the heating (Chinese et al., 2011) or ventilation (Caputo & Pelagagge, 2009) plant. In (Noro et al., 2022a), an optimization of the main parameters of a hybrid condensing radiant tubes system coupled to a heat pump to heat a typical industrial building was modeled in three climatic zones of Italy using dynamic simulation software.

In an industrial building, there are specific characteristics: generally there is some equipment on the walls or on the ceiling such as tubes, bridge cranes, pipes, etc.; there are large doors (often open), high heights (7 m or more), scarce thermal insulation, and large floor surfaces with different types of occupation by workers (Noro et al., 2022b). These are the main reasons for which different climatization plants are used instead of traditional ones: high and medium temperature radiant heating systems are quite common. Water strips are medium-temperature systems made up of iron tubes welded to a plate. Water at medium temperature (typically 60–90 °C) crosses the tubes and exchanges heat with the indoor environment both by radiation and convection. Usually, the former account for the greatest part of the heat transferred by the plate to the environment, but the latter can play an important role because of the non-negligible contribution of the natural convection.

CONTACT Marco Noro ✉ marco.noro@unipd.it 🏢 Department of Management and Engineering, University of Padua, Stradella S. Nicola, 3, Vicenza 36100, Italy

Reviewing editor: Michelle Bloor SChool of Earth and Environmental Science Scotland's Rural College UK

Usually, performance of water strips are provided by the manufacturer at nominal condition fixed by the EN 14,037 standard (European Committee for Standardization, 2016). Such internal nominal conditions do not usually correspond to the real operation of an industrial building: a constant movement of air can be expected, for example, by means of a ventilation system. More generally, the presence of doors, windows, or skylights and indoor air evacuation towers can induce air flow, especially during winter when the temperature difference between the inside and outside of the shed is relevant. As the main novelty of this study, a calculation procedure is developed to evaluate the increase in the yield of the water strips heating system in real operation conditions with respect to the standard according to EN 14,037.

The authors refer to a commercially available water strip model, which is assumed to be used varying some boundary conditions, such as the convective heat transfer coefficient between the heating water strips and the internal air and the presence or absence of anticonvective flashing.

Regarding the first point, various studies are present in the literature whose references are considered in the present study, but, to the best knowledge of the authors, none of these specifically refers to water strips in industrial buildings. Instead, they refer to heating or cooling systems that are somewhat similar to these.

The first studies on the effects of the variation of some parameters on the heat exchange of the surfaces of indoor spaces date back to the 1950s. Schutrum and Vouris (1954), for example, experimentally measured the effect of the room size and the non-uniformity of the temperature of the heating surfaces on the yield of these surfaces. They obtained a marginal effect for the former; instead, for the latter, they highlighted a yield of the panels, both ceiling and on the floor, equal to that which would have occurred with the entire surface heated to a uniform temperature equal to the weighted average with the heated and unheated surface areas.

In Min et al. (1956), some equations for the natural convection coefficients have been provided in the case of radiant ceiling panels. More recently, Awbi and Hatton have carried out numerous measurement campaigns to develop equations for the calculation of the heat transfer coefficients for both natural (Awbi & Hatton, 1999) and mixed (natural+forced) (Awbi & Hatton, 2000) convection. However, in this case, the measurements were performed in a very small room. In (Abdul-Jabbar, 2001), an extensive review on the determination of the convective heat transfer coefficients of surfaces in two and three dimensions was carried out. In this study, the authors highlighted the wide variety of values that can

be determined as a function of the different heat transmission configurations (width, position, temperature of the heated surface, etc.). To the best knowledge of the authors, none of the previous work has determined some relationships to quantify the effects of air flow near hot water strip systems that hang from the ceiling. Two works have been carried out in this regard (Jeong & Mumma, 2003; Novoselac et al., 2006), but they are focused on ceiling panels for cooling. Hence, the reason for this work is the purposes listed above.

The study has been conducted in two steps. In the first part, the analysis is carried out under steady-state conditions. In the second part of the paper, a numerical analysis using computational fluid dynamics (CFD) is reported to validate the thermal performance of the water strips under real operating conditions determined by the simplified method described in the first part. Due to computational effort, the analysis is conducted using a two-dimensional model of an industrial shed. The effectiveness of the use of the water strips heating system is demonstrated in operating conditions with air flow.

2 Methods

2.1 Building modelling

The industrial building (type of use E.8 by the Italian decree DPR 412/93) (Italian Government, 2022) is located in the province of Cuneo (North-West of Italy), latitude 44°36' N, altitude 404 m above sea level, 2814 degree days (climatic zone E (Italian Government, 2022)). The heating period is from 15th September till 30th April. The thermal transmittances expressed in W m^{-2} K^{-1} are: 0.389 for external wall, 0.128 for the floor facing ground, 4.086 for ceiling, 0.208 for ceiling shed, 5.0 for windows.

The building is divided into two thermal zones (Figure 1) whose main characteristics are reported in Table 1 (Lazzarin & Noro, 2020). In this study, we refer only to thermal zone 1.

2.2 Steady-state calculus procedure

Here it is reported the calculus procedure to evaluate the total heat power (convective + radiative) exchanged by the water strips considering the real operating conditions instead of the standard conditions. Real operating conditions are simulated by varying the convective heat transfer coefficient between indoor air and water strip (see section 2.2.6). Instead, standard operating conditions are reported in EN 14,037 standard (European Committee for Standardization, 2016), where the test method and the test installation to determine the thermal output
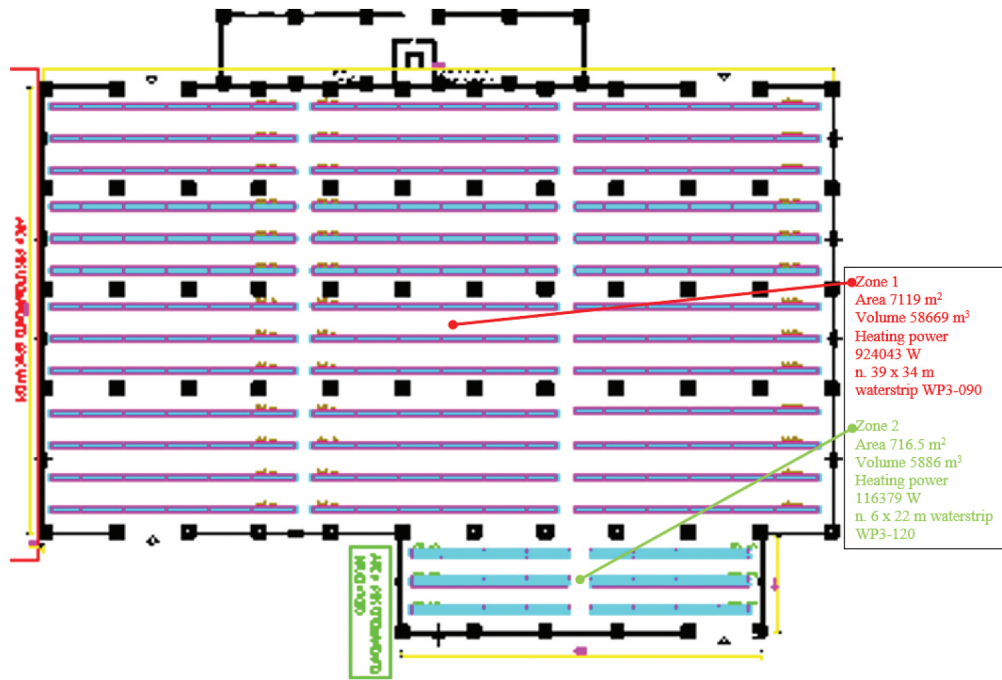
Figure 1. Factory shed used in the present study [20].

Table 1. Thermal zones of the building

	Thermal zone 1	Thermal zone 2
Floor area (m^2)	7119	716.5
Net height (m)	8.24	8.22
Indoor air temp. (°C)	18	18
Net volume (m^3)	58669	5886

of pre-fabricated ceiling mounted radiant panels are described. The standard conditions of the tests defined in (European Committee for Standardization, 2016) are here briefly reported:

- the booth for testing ceiling mounted radiant panels has 4 m × 4 m × 3 m inside dimensions, and air infiltration has to be limited at all;
- all six surrounding surfaces have an emissivity of minimum 0.9, and they are chilled to keep the difference between them and the average temperature of all six surfaces not higher than 0.5 K;
- the temperatures of air and all six surrounding surfaces are fixed at 20 °C.

1 Hollow painted shaped sheet metal (Lower part - Front)
2 Tubes
3 Reinforcement cross tube
4 Top insulating panel (Upper part- Back)
5 Flashing presence
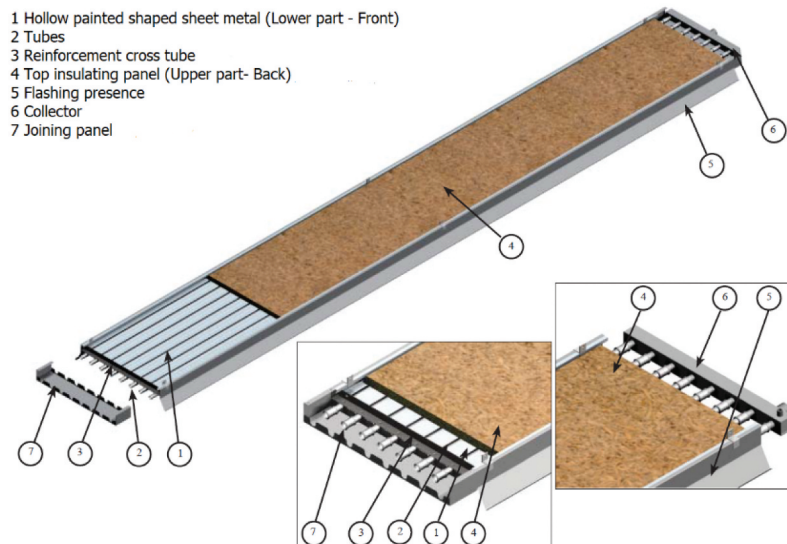6 Collector
7 Joining panel

Figure 2. Main elements of the water strip (courtesy of Officine Termotecniche Fraccaro srl).

In this study, heat flux is expressed in watts per meter of linear length of the water strip, as it is referred to a strip having a width of 0.9 m (Figure 2 reports the main elements of the water strip).

2.2.1 Calculus of the average temperature of the hot water flow

The average value of the temperature of the hot water flow ($T_{f,avg}$) is calculated based on the difference between this temperature and that of indoor air T_{ai} (ΔT_m) (with $T_{ai} = 15$ °C) (ΔT_m is considered to vary in the 30–90 °C range following the available performance data of the water strip) (Officine Termotecniche Fraccaro, 2017):

$$T_{f,avg} = \Delta T_m + T_{ai} \tag{1}$$

2.2.2 Calculus of the average temperature of the lower side (front) water strip (plate)

The average temperature of the lower side (front) water strip (plate) $T_{p,front,avg}$ is calculated based on the average temperature of hot water $T_{f,avg}$ on the basis of data in the literature (Lazzarin & Crose, 2000) (Figure 3).

2.2.3 Calculus of the average temperature of the upper side (back) water strip (plate)

The average temperature of the upper side (back) water strip (plate) $T_{p,back,avg}$ is calculated as a function of the presence of thermal insulation and

based on literature reference data (Lazzarin & Crose, 2000):

$$T_{p,back,avg} = IF(THERMAL\ INSULATION \\ = YES; 0.37; 0.52) \cdot T_{p,front,avg} \tag{2}$$

2.2.4 Calculus of the mean radiant temperature of thermal zone 1

The mean radiant temperature of thermal zone 1 (T_{mr}) is determined as the weighted average (where the weights are the areas A_k) of the internal surface temperatures T_{sk}, considering that all surfaces have the same emissivity (0.9):

$$T_{mr} = \frac{\sum_k A_k \cdot T_{sk}}{\sum_k A_k} \tag{3}$$

T_{mr} is calculated on the basis of the thermal transmittance values U_e and the outdoor design air temperature θ; suitable external and internal convective heat transfer coefficients are established ($\alpha_e = 25$ W m^{-2} K^{-1} and α_i (Spiga, 2018), respectively):

$$\alpha_{ik} \cdot (T_{ai} - T_{sk}) = U_e^* \cdot (T_{sk} - \theta) \rightarrow T_{sk} \\ = \frac{\alpha_{ik} \cdot T_{ai} + U_e^* \cdot \theta}{U_e^* + \alpha_{ik}} \tag{4}$$

where $U_e^* = \frac{1}{\frac{1}{U_e} + \frac{1}{\alpha_e}}$ is the thermal transmittance taking into account the external convective heat transfer coefficient. Based on the data reported in Spiga (2018), the results are as follows:

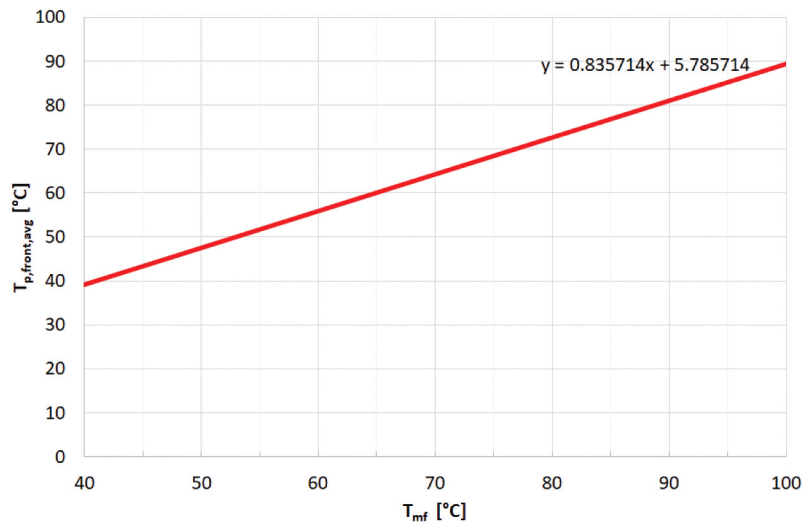$$T_{mr,zone1} = 11.4°C \quad T_{mr,zone2} = 10.6°C \tag{5}$$

Figure 3. Average temperature of the front plate (Tp,front,avg) as a function of the average temperature of the hot water temperature (Tmf).

2.2.5 Calculus of the radiant heat flux exchanged by the lower and upper parts of the plate

The radiant heat flux exchanged by the lower ($q_{r,front}$) and the upper part ($q_{r,back}$) of the plate are (L is the length of the plate) are calculated as follow:

$$q_{r,front} = 5.67 \cdot 10^{-8} \cdot 0.95 \cdot L$$
$$\cdot \left(T_{p,front,avg}^4 - T_{mr,zone1}^4\right) (\text{W/m}) \qquad (6)$$

$$q_{r,back} = 5.67 \cdot 10^{-8} \cdot 0.95 \cdot L$$
$$\cdot \left(T_{p,back,avg}^4 - T_{mr,zone1}^4\right) (\text{W/m}) \qquad (7)$$

2.2.6 Calculus of the convective heat transfer coefficient between indoor air and water strip

The coefficient of convective heat transfer between indoor air and the lower part (front) ($\alpha_{conv,front}$) and the upper part (back) ($\alpha_{conv,back}$) of the water strip is calculated according to the references reported in Table 2.

Case n. 1 and n. 4 represent the heat convection between the water strip and the indoor air without induced air flow (i.e. natural heat convection), case n. 1' and 4' represent the same equations considering some induced air flow (that is, opening a door on a lateral wall, opening a skylight, or activating an outlet turret on the shed roof, activating the ventilation plant with an air change rate of 0.5 vol h^{-1}). In the latter cases, an increase of 30% of the convective coefficient $\alpha_{conv,front}$ is supposed, based on the reference (Min et al., 1956) where an increase of 60% of the convective coefficient is fixed with an air change rate of 1 vol h^{-1}.

Case n. 5 represents the heat convection between the water strip and the indoor air with induced air flow as forced heat convection with an air velocity of 1 m s^{-1}.

2.2.7 Determination of the convective thermal power exchanged by the water strip

The convective thermal power exchanged by the lower ($q_{conv,front}$) and the upper ($q_{conv,back}$) part of the water

strip, with and without flashing presence (flashing is supposed to reduce convective heat transfer by 25% (Lazzarin & Crose, 2000)) is calculated as follows:

$$q_{conv,front} = IF(FLASHING\,PRESENCE = YES; 0.75; 1)$$
$$\cdot \alpha_{conv,front} \cdot L \cdot \left(T_{p,front,avg} - T_{ai}\right) (\text{W/m})$$
$$\qquad (8)$$

$$q_{conv,back} = IF(FLASHING\,PRESENCE = YES; 0.75; 1)$$
$$\cdot \alpha_{conv,back} \cdot L \cdot \left(T_{p,back,avg} - T_{ai}\right) (\text{W/m})$$
$$\qquad (9)$$

2.2.8 Calculus of the radiant, convective and total thermal power exchanged by the water strip

The radiant ($q_{r,tot}$), convective ($q_{conv,tot}$) and total (q_{tot}) thermal power exchanged by the water strip are calculated as follows:

$$q_{r,tot} = q_{r,front} + q_{r,back} (\text{W/m}) \qquad (10)$$

$$q_{conv,tot} = q_{conv,front} + q_{conv,back} (\text{W/m}) \qquad (11)$$

$$q_{tot} = q_{r,tot} + q_{conv,tot} (\text{W/m}) \qquad (12)$$

2.3 Unsteady state numerical analysis

In this section, the thermofluid dynamic analysis for the water strips heating system developed in Ansys Fluent® (rel. 18.2) is reported. The conditions investigated, the geometric model, the calculation grid generated, and the boundary conditions are analyzed. In section 3.2 the results are presented and discussed.

As the study is under transient conditions ('unsteady'), a sensitivity analysis was preliminarily performed to identify the optimal time step to be set. Since the operating conditions feature convective air flow due to density gradients (temperature) and radiative heat exchange, it was necessary to set the time step on the order of a hundredth of a second.

Table 2. Equations for the calculation of the convective heat transfer coefficient

Case nr.	Type of convection	Equation	Reference
1	Natur. Conv. (Front)	$\alpha_{conv,front} = 0.59 \cdot ((T_{p,front,avg} - T_{ai})/D_e)^{0.25}$	(Lazzarin & Crose, 2000) (p. 344) (Lazzarin, 2002) (p. 240)
2	Natur. Conv. (Front)	$\alpha_{conv,front} = 0.71 \cdot ((T_{p,front,avg} - T_{ai})/D_e)^{0.25}$	(Brunello et al., 1993) (p. 23)
3	Natur. Conv. (Front)	$\alpha_{conv,front} = 0.87 \cdot ((T_{p,front,avg} - T_{ai})^{0.25}) * (4.91/D_e)^{0.25}$	(ASHRAE HANDBOOK, 2020) (Eq. (10))
4	Natur. Conv. (Front)	$\alpha_{conv,front} = 1.736 \cdot (T_{p,front,avg} - T_{ai})^{0.16}/D_e^{0.52}$	(Lazzarin & Noro, 2020)
5	Forced Conv. (Front)	$\alpha_{conv,front} = (0.0296 \cdot (w \cdot 0.3/1.644e-5)^{0.8}) \cdot 0.0266/0.3$	(Bonacina et al., 1992) (p. 279)
1' – 2' – 3' – 4'	Natur. Conv. Coefficient increase due to outdoor air exchange rate	$\alpha'_{conv,front} = 1.3\,\alpha_{conv,front}$ (based on the increase of 60% @ 1 vol/h, 0 °F)	(Awbi & Hatton, 1999)
-	Natur. Conv. (Back)	$\alpha_{conv,back} = 1.32 \cdot ((T_{p,front,avg} - T_{ai})/D_e)^{0.25}$	(Lazzarin & Crose, 2000) (p. 344)

Five values were tested: 0.1, 0.05, 0.025, 0.01, 0.005 s. With time steps of 0.1 and 0.05 s, the solution diverged. Therefore, the value of 0.01 s was finally fixed as the best trade-off between computational effort and the accuracy of the solution. The 'unsteady' simulation lasted when the curve of the specific power (in watt per meter) exchanged by the plates as a function of time reached an asymptotic value (see section 3.2).

Radiation was considered by implementing the 'Surface-to-Surface, S2S radiation' model (ANSYS FLUENT, 2022). Two cases were simulated: for case 1 (negligible air flow, natural convection), air flow was simulated by setting the 'laminar' model. For case 2 (constant air flow, forced convection), activation of the k-ε turbulence model was considered (Launder & Spalding, 1972).

2.3.1 Case 1: Radiation and natural convection

As shown in Figure 4, a two-dimensional section of the industrial shed of reference (Lazzarin & Noro, 2020) was modeled. The shed was approximated with a double trapezoid, each with a smaller base, a higher base and height of 8.0 m, 9.5 m and 6 m, respectively. The water strips of 0.9 m width and 0.1 m height were placed with a pitch of 3 m as shown in Figure 4a. As a consequence, a 12 m wide shed has 3 plates.

The mesh obtained by the geometric model features cells in a square or rectangular shape, with a maximum size of 0.05 m. Near the water strip plates, the calculation grid was thickened by means of a refinement procedure. The mesh sensitivity analysis demonstrated that the optimal mesh configuration shows the best compromise between the accuracy of the solution and the computational effort, and it is made up of about 22,000 elements (Figure 4b).
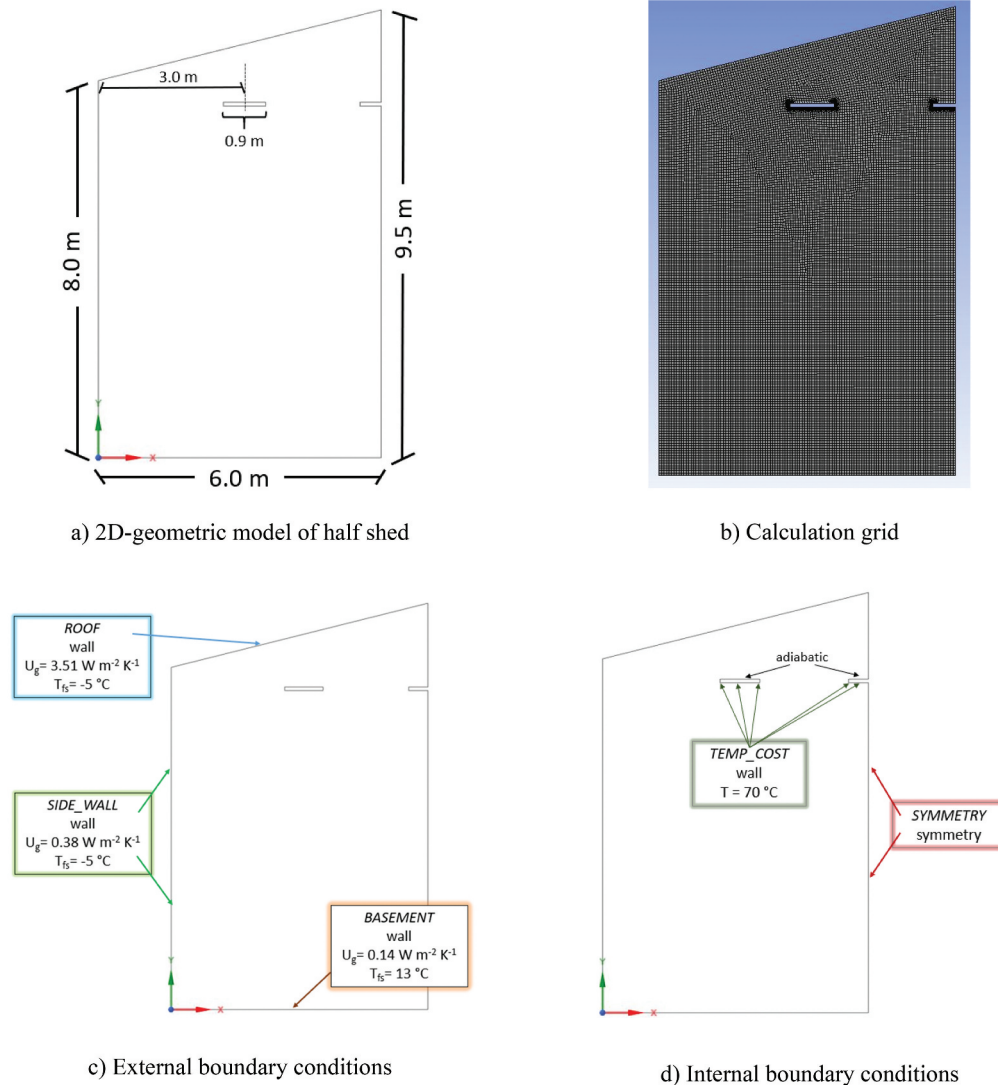

a) 2D-geometric model of half shed

b) Calculation grid

c) External boundary conditions

d) Internal boundary conditions

Figure 4. The model of the shed building for case 1.

Figure 4c shows the boundary conditions applied to the external edges of the geometric model in terms of global transmittance of the walls (U_{wall}). They already take into account the conductive resistance through the walls and the convective resistance on the external side. By defining T_{wall} as the internal temperature of each edge, L as its length, and T_{fs} as the temperature of the external fluid, the software takes into account the specific average power per linear meter q_{wall} for each side, using the following equation:

$$|q_{wall}| = |U_{wall}L(T_{wall} - T_{fs})| \qquad (13)$$

To keep the outline of any symmetries, it is necessary to identify the axis of symmetry and assign the suitable condition (Figure 4d).

Three sides of the strip (lower base and the two heights) were kept at a constant temperature of 70 °C (average operating temperature). On the contrary, the adiabatic condition was assigned to the upper side, thus simulating a thermal insulated water strip.

2.3.2 Case 2: Radiation and forced convection

Figure 5a shows the geometry used for the system performance analysis in the case of a constant air flow inside the building. There is an opening of 0.6 m height on the bottom left, from which external air enters the shed. On the top right, an opening of 0.3 m width is placed (i.e. half of the radius of a 0.6 m diameter suction tower placed on the roof). Forced convection is simulated by imposing a constant mass flow (or air speed) at the outlet ('Outlet' in Figure 5c).

With regard to the generation of the mesh, the same considerations and hypotheses as previously described can be considered. In addition to the boundary conditions already shown in Figure 4, the insertion of a pressure inlet (for the 'Inlet' section) and a negative velocity inlet (for the 'Outlet' section) is considered

(Figure 5c). The renewal air temperature is set at 13 °C, taking into account the enthalpy contribution of any heat recovery unit (a typical situation in industrial environments).

3 Results and discussion

3.1 Steady-state analysis results

The results are reported in Figure 6 in terms of thermal power expressed in watt per meter of linear length exchanged by the water strip (section 2.2.8) for the different cases described in the previous section (Table 2). The performance stated by the manufacturer of the water strips is also reported (last graph in Figure 6). The main results that can be deduced by comparing the graphs in Figure 6 are:

- in all the cases, the greatest part is the radiant heat flux exchanged by the lower part of the plate (say from 50% to 85%). Nevertheless, the second largest contribution is due to the convective heat flux by the lower part, that can weight from 10% till 40%. The convective contribution increases with the increase of ΔT_m (i.e. feeding the water strips with higher average temperature of the hot water flow) and when passing from Case 1 (natural convection) to Case 5 (forced convection);
- the equation that approximates in the best way the real performance of the water strip is that of case 2' ($\alpha_{conv,front} = 0.71.((T_{p,front,avg} - T_{ai})/D_e)\cdot0.25$ (Brunello et al., 1993)) with a multiplying coefficient of 30%. In fact, by comparing the 'power' equations reported on the graphs, it can be deduced that the one related to case 2' allows the best approximation of that of the EN 14,037 standard to evaluate thermal performance as a function of ΔT_m:

a) 2D-geometric model of half shed   b) Calculation grid   c) Boundary conditions
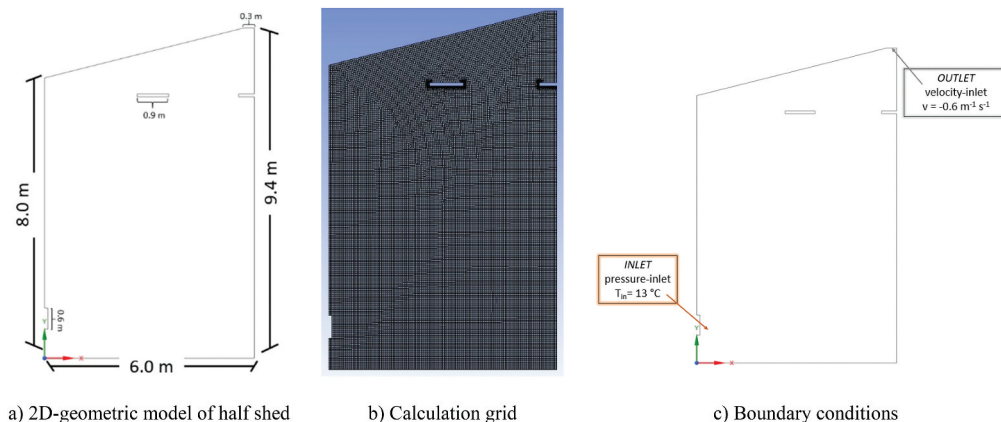
Figure 5. The model of the shed building for case 2.

$$q_{tot} = K(\Delta T_m)^n \qquad (14)$$

As a matter of fact, this corresponds to the increase of the convective heat transfer coefficient when the water strip operates under real conditions with respect to the EN 14,037 test conditions. Furthermore, the effectiveness of the case 2 equation is confirmed by using the equation in EN 14,037 test conditions (Figure 7): the blue curve (q_{tot}), and so the relative 'power' equation, can approximate quite well that of the water strip producer (last graph in Figure 6);

- the flashing presence on the lower part and thermal insulation presence on the upper part of the water strip reduce the thermal power. This is due to

a decrease in the convective heat transfer on both sides of the plate for the flashing, and of the convective and radiation heat transfer on the upper side for the thermal insulation.

3.2 Unsteady-state analysis results

Referring to section 2.3, the results of case 1 are first reported. As shown in Figure 8, the simulation was stopped when the curve that interpolates the values of the specific heat flow exchanged over time by the single plate reached an almost constant value. The latter is equal to about 400 W m^{-1}: at 800 s a value of 399 W m^{-1} is returned, at 1200 s 397 W m^{-1}, that is, a deviation of 0.5%.
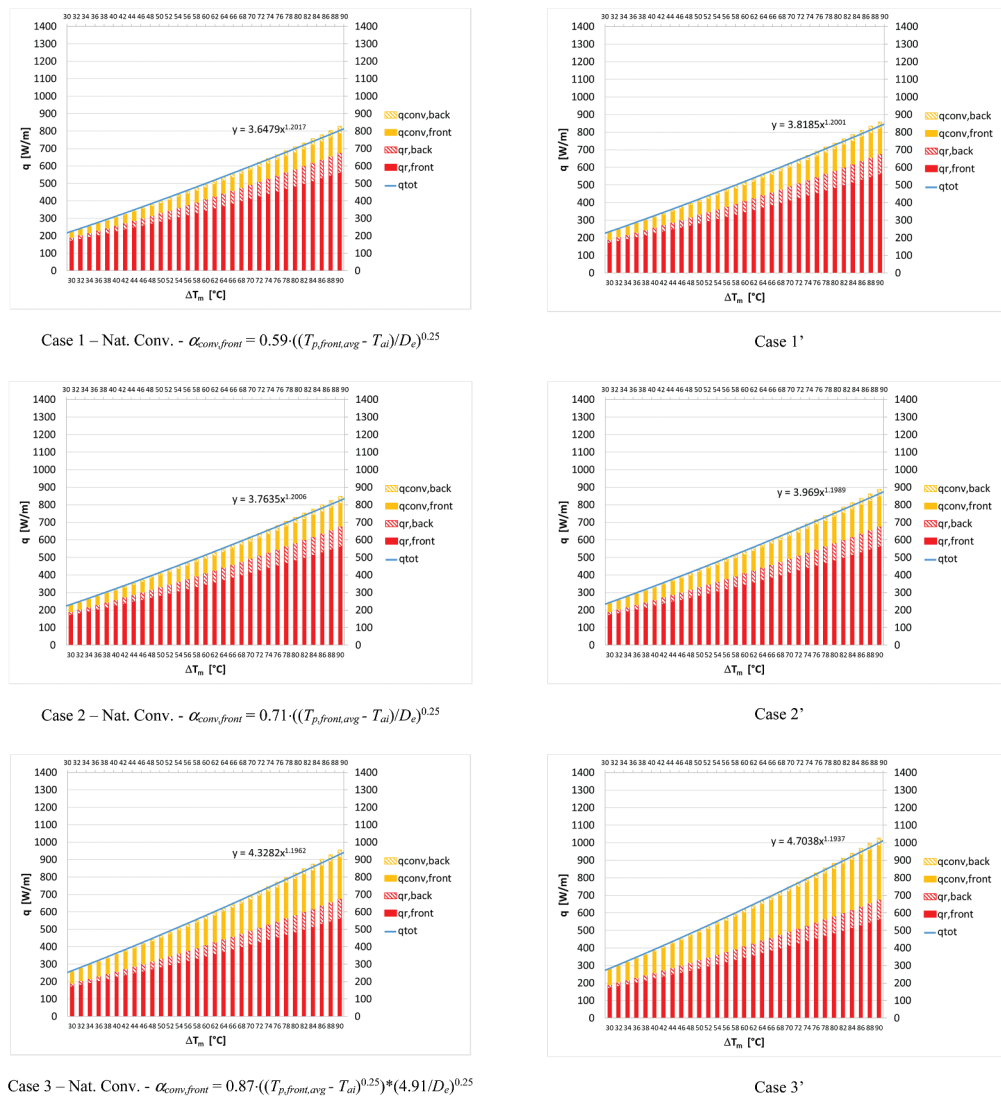

Figure 6. Thermal power exchanged by the water strip without flashing and with thermal insulation for the cases considered in Table 2. Heat flux is expressed in watts per meter of linear length of the water strip, as it is referred to a strip having a width of 0.9 m. The last graph reports the performance of the water strip according to the EN 14,037 standard but without thermal insulation in the collectors (HLK test center, 2020) and the performance determined using the formula of case 2' in the operating conditions of EN 14,037.
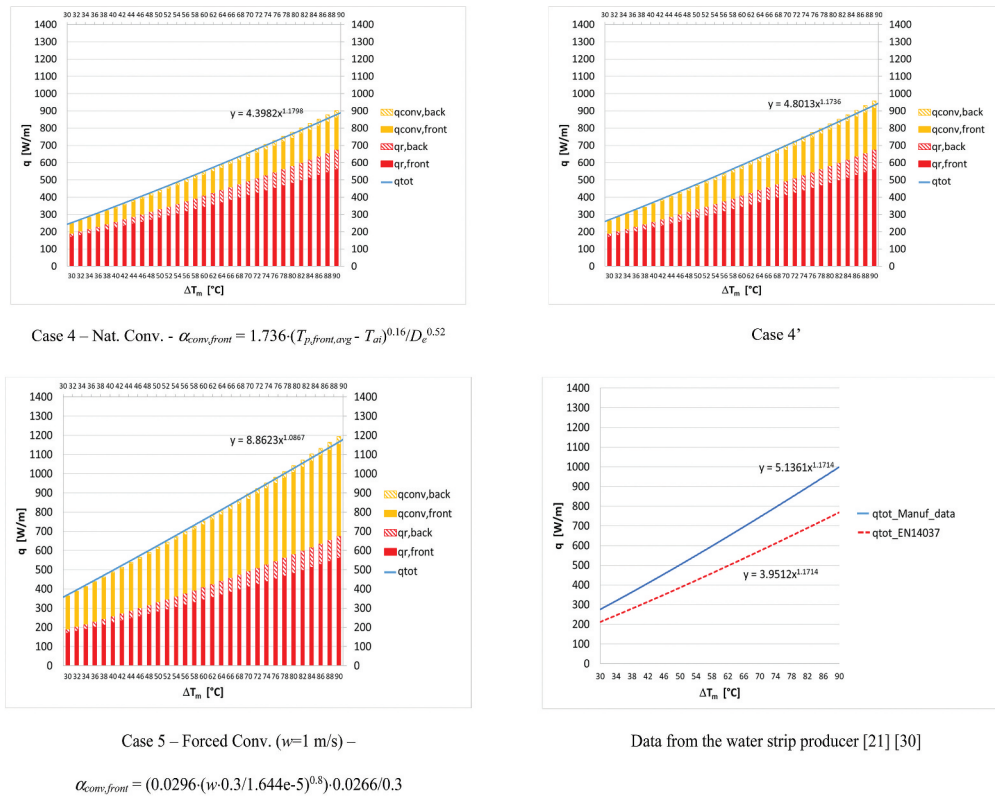
Case 4 – Nat. Conv. - $\alpha_{conv,front} = 1.736 \cdot (T_{p,front,avg} - T_{ai})^{0.16}/D_e^{0.52}$

Case 4'

Case 5 – Forced Conv. (w=1 m/s) –

$\alpha_{conv,front} = (0.0296 \cdot (w \cdot 0.3/1.644\text{e-}5)^{0.8}) \cdot 0.0266/0.3$

Data from the water strip producer [21] [30]

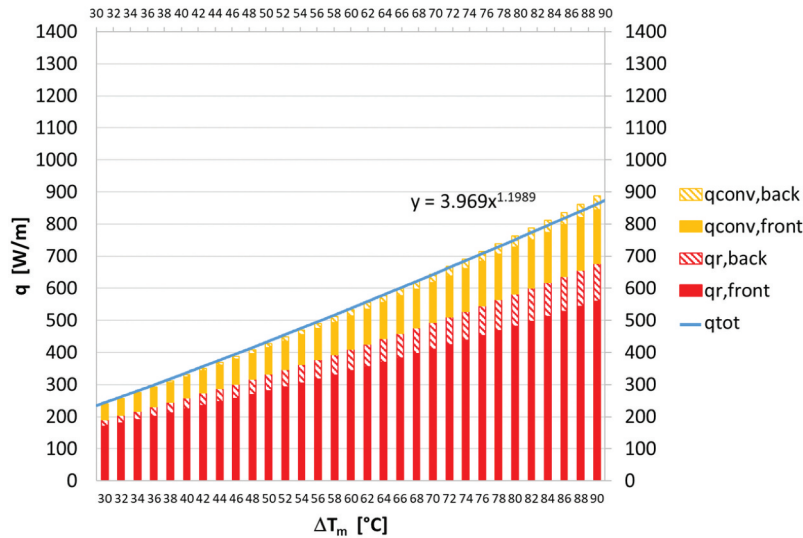**Figure 6.** (Continued).

Figure 7. Thermal power exchanged by the water strip (expressed in watts per meter of linear length of the water strip, as is referred to a strip of 0.9 m width) with no flashing presence and with thermal insulation for the operating conditions of the EN 14,037 standard.

The air temperature and velocity fields for case 1 were also investigated. The analysis was carried out assuming an initial temperature ($t = 0$ s, inactive plate) of 15 °C (Figure 9a). After activation of the water strip system, a stratification of temperature is created inside the industrial shed due to natural convection: the air closest to the work area reaches a temperature around 15.50–17.50 °C, while the air closest to the radiant plates is around 24–26 °C (Figure 9b). At the same time, natural convection induces a continuous local mixing of air that is more
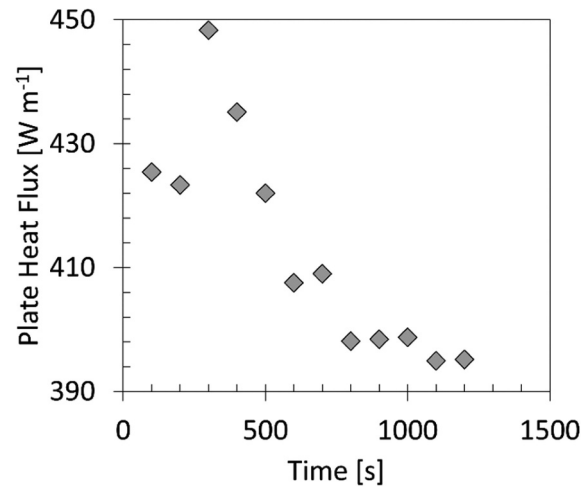
Figure 8. Case 1, specific thermal power exchanged by the water strip.

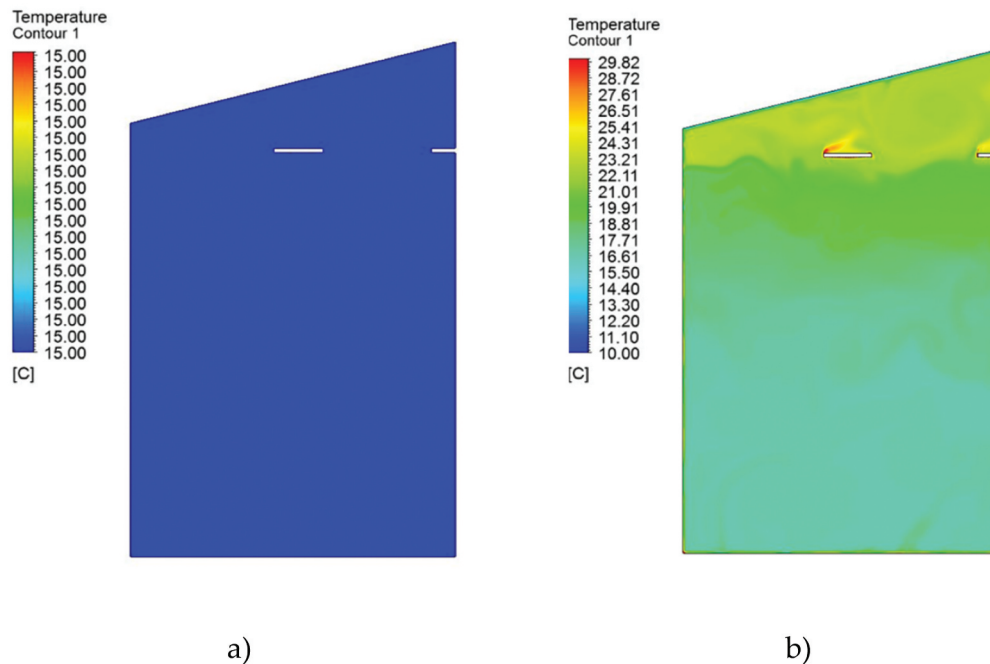a)   b)

Figure 9. Case 1, contour indoor air temperature: a) 0 s; b) 1000 s.

intense near the hottest surfaces (Figure 10). In the stratified zone at higher temperature, a speed of 0.33 m s^{-1} can be reached.

In the case of forced convection (case 2), Figure 11 shows the flow field with the activation of the water strip plates. After 700 s, it can be said that the flow is completely stabilized. The air exiting at a constant speed from the outlet causes external air to be sucked into the building. Air flow tends to increase in the symmetrical section of the shed due to suction of the tower on the roof. The obstacle

due to the presence of radiating plates forces the air to divert its trajectory (Figure 11b,c).

In Figure 12a, the speed vectors oriented towards the right near the inlet, indicating the entry of fresh air, and vectors oriented upward near the outlet, indicating the air outlet, are reported. Due to continuous air exchange, the temperature within the plant tends to uniform around a value of 15–16 °C (Figure 12b).

It is worth observing that, in terms of the specific power exchanged by the water strips in conditions of
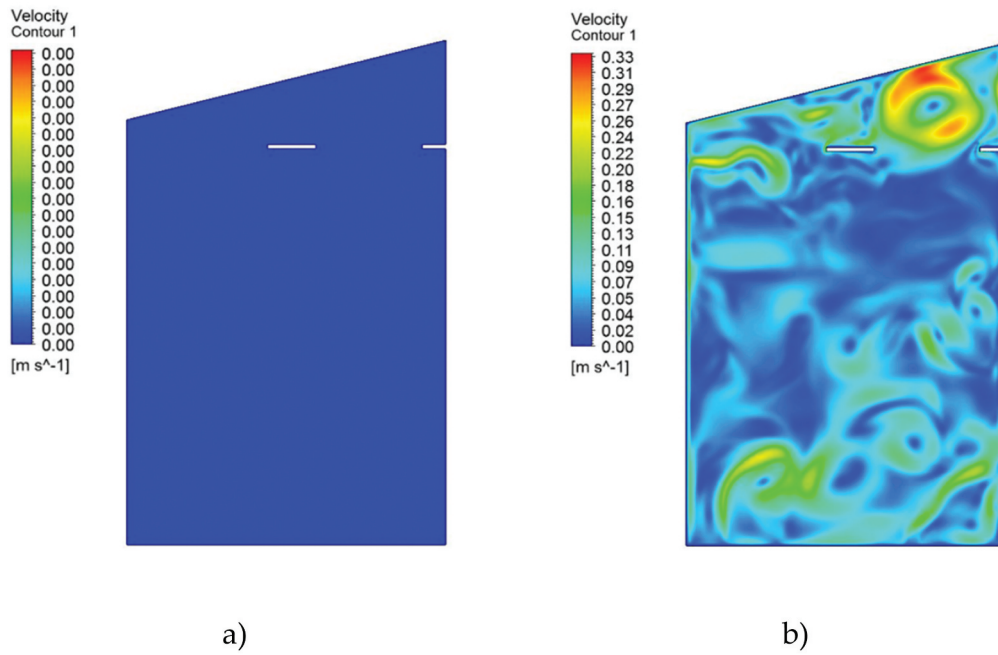
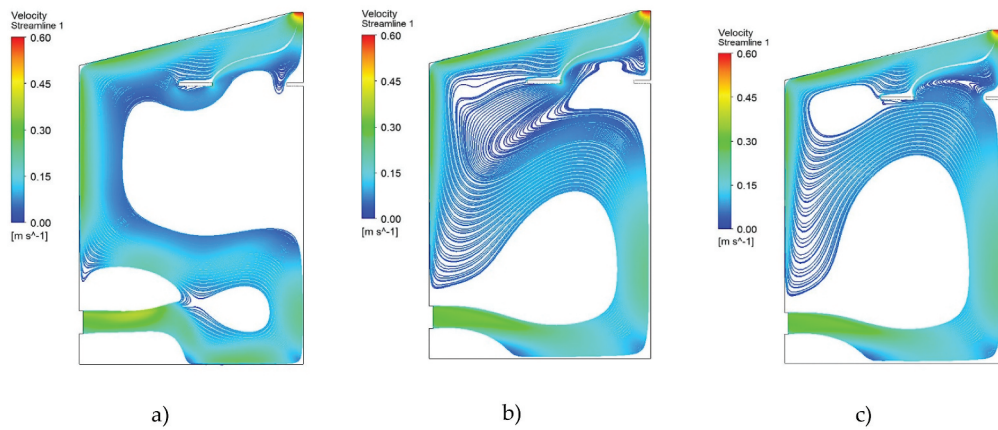**Figure 10.** Case 1, contour indoor air velocity: a) 0 s; b) 1000 s.

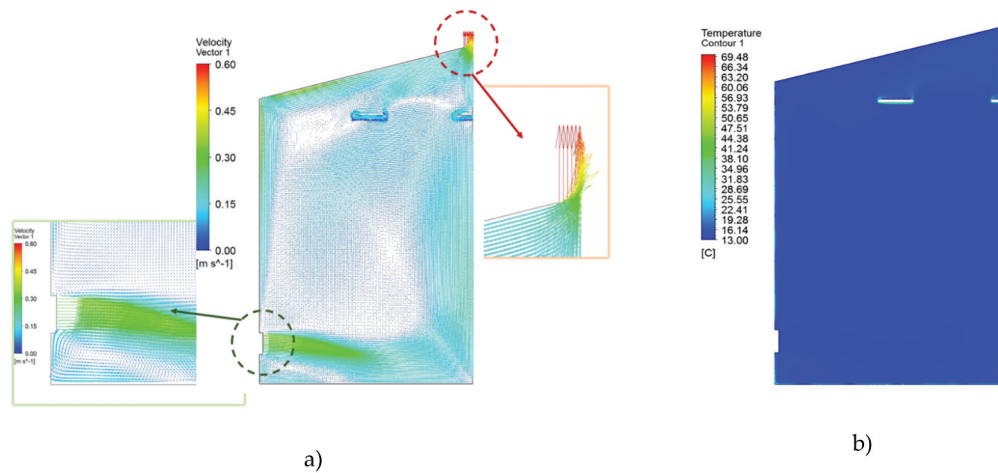**Figure 11.** Case 2, flow lines: a) 100 s; b) 400 s; c) 700 s.

Figure 12. Case 2: a) Velocity vectors: t = 700 s; b) Contours indoor temperature: t = 700 s.
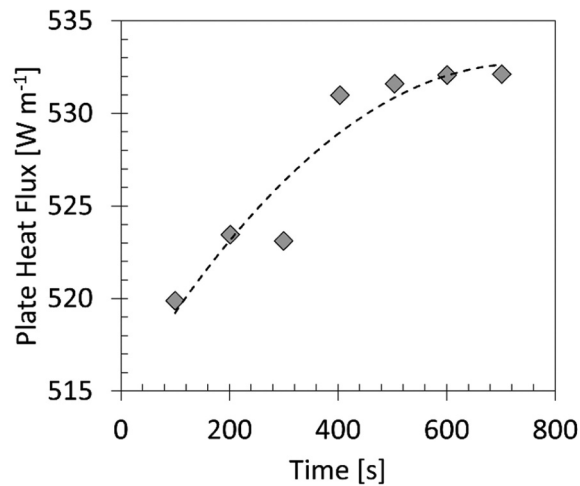
Figure 13. Case 2, specific thermal power exchanged by the water strip.

constant air flow, a value of just over 530 W m^{-1} is reached (Figure 13). This value is approximately 33% higher than that estimated for case 1 (Figure 8).

4 Conclusions

The analysis carried out in the first part of this study, based on the reference literature, allows to give some remarks:

- the estimation of the increase of the convective heat transfer coefficient of the water strip heating system in normal operating conditions (i.e. the presence of induced air flow near the radiant panels due, for example, to the opening of a door on a side wall, or to the opening of a skylight on the roof, or to the operation of the ventilation system with air change flow of 0.5 vol h^{-1}) is in the order of 30%–40% compared to the operating conditions of the EN 14,037 standard;
- considering that convective heat transfer weighs for a percentage variable between 35% and 45% of the total thermal output of the water strip (depending on the model and the ΔT_m), an increase of the overall yield in the order of at least 10%–20% compared to the data stated according to the EN 14,037 standard is surely achievable;
- furthermore, in real operating conditions, the water strips 'see' internal surface temperatures that probably are not uniform and lower than the internal air temperature, which commonly is around 20 °C (i.e. the test conditions according to EN 14,037);
- in the case of non-insulated water strips, there is a further exchange of thermal power with the

environment, as can be seen from the data measured in the test room according to the EN 14,037 standard (blue curve in the last graph of Figure 6; HLK test center, 2020).

It can be concluded that the increase in the overall yield of the heating strips, compared to the data measured according to the EN 14,037 standard, can be at least of the order of 30%. This result has been verified by means of CFD simulations. Two case studies were modeled and simulated. The main remarks are:

- numerical results for the configuration studied confirm that the presence of constant air exchange leads to an improvement of more than 30% in the performance of the water strip system;
- it is reasonable to think that other situations of real operation of the system in industrial sheds (such as the opening of doors, windows, or skylights, the presence of hoods or ventilation towers for internal air, and the temperatures of the internal surfaces that are not uniform and certainly lower than that of the internal air) can lead to a similar or even greater increase, in the order of 30%–40%, of the yield of the water strips.

Based on these first results, as a further development of this work, a dynamic simulation model of the system will be developed, with the scope of optimizing the size and the operational parameters (such as the feed water temperature) of the water strip heating system. An economic analysis will be useful to assess the economic viability of the proposed energy system and its profitability compared to conventional technologies.

Nomenclature

Symbol	Meaning	Unit
A	Area	m^2
D	Diameter	m
L	Length	m
q	Thermal power	$W\ m^{-1}$
T	Temperature	°C
U	Thermal transmittance	$W\ m^{-2}\ K^{-1}$
w	Velocity	$m\ s^{-1}$

Greek symbol

α	convective heat transfer coefficient	$W\ m^{-2}\ K^{-1}$
θ	outdoor design air temperature	°C

Subscript

ai	air indoor
avg	average
back	back
conv	convection
e	external
f	flow
fs	external fluid
front	front
i	internal
k	counter
m	medium
mr	mean radiant
p	plate
rad	radiation
s	surface
wall	wall
zone	zone

Acknowledgements

Disclosure statement

No potential conflict of interest was reported by the authors.

Data availability statement

The data that support the findings of this study are available from the corresponding author, M.N., upon reasonable request.

References

Abdul-Jabbar, N. K. (2001). Natural convective heat transfer coefficient – a review. *Energy Conversion and Management*, *42*(4), 505–517. https://doi.org/10.1016/S0196-8904(00)00043-1

ANSYS FLUENT 12.0/12.1 Documentation, https://www.afs.enea.it/project/neptunius/docs/fluent/html/ug/node1484.htm (Retrieved September 16, 2022).

ASHRAE HANDBOOK HVAC Systems and Equipment, 6.3, Equation (10), 2020.

Awbi, H. B., & Hatton, A. (1999). Natural convection from heated room surfaces. *Energy and Buildings*, *30*(3), 233–244. https://doi.org/10.1016/S0378-7788(99)00004-3

Awbi, H. B., & Hatton, A. (2000). Mixed convection from heated room surfaces. *Energy and Buildings*, *32*(2), 153–166. https://doi.org/10.1016/S0098-8472(99)00063-5

Bonacina, C., Cavallini, A., & Mattarolo, L. (1992). Trasmissione del calore. *Cleup*, 279. 8871789202.

Brunello, P., Cavallini, A., & Zecchin, R. (1993). Moduli stagni a gas con tubi radianti. *SGE*, 23.

Caputo, A. C., & Pelagagge, P. M. (2009). Upgrading mixed ventilation systems in industrial conditioning. *Applied Thermal Engineering*, *29*(14–15), 3204–3211. https://doi.org/10.1016/j.applthermaleng.2009.04.025

Chinese, D., Nardin, G., & Saro, O. (2011). Multi-criteria analysis for the selection of space heating systems in an industrial building. *Energy*, *36*(1), 556–565. https://doi.org/10.1016/j.energy.2010.10.005

European Committee for Standardization. EN 14037-2:. 2016, Free hanging heating and cooling surfaces for water with a temperature below 120 °C. Part 2: Pre-fabricated ceiling mounted radiant panels for space heating — Test method for thermal output (Retrieved December 15, 2022)

HLK test center (IGTE, University of Stuttgart), 2020, Test Report n. DC520 D12.5273, n. DC520 D12.5274.

Italian Government. DPR 26 Agosto 1993, n. 412, Regolamento Recante Norme per la Progettazione, L'installazione, L'esercizio e la Manutenzione Degli Impianti Termici Degli Edifici ai Fini del Contenimento dei Consumi di Energia, in Attuazione Dell'art. 4, Comma 4, Della Legge 9 Gennaio 1991, n. 10, Available online: (Retrieved October 18, 2022) https://www.gazzettaufficiale.it/eli/id/1993/10/14/093G0451/sg

Jeong, J. W., & Mumma, S. A. (2003). Ceiling radiant cooling panel capacity enhanced by mixed convection in mechanically ventilated spaces. *Applied Thermal Engineering*, *23*(18), 2293–2306. https://doi.org/10.1016/S1359-4311(03)00211-4

Katunska, J., Oberleova, J., Rusnak, A., & Toth, S. (2014). Diagnosis of elected industrial hall object and idea for its reconstruction. *Advanced Materials Research*, *1057*, 19–26. https://doi.org/10.4028/www.scientific.net/AMR.1057.19

Launder, B. E., & Spalding, D. B. (1972). *Lectures in Mathematical Models of Turbulence*. Academic Press.

Lazzarin, R. (2002). *Intervista sul riscaldamento degli ambienti nell'industria* (2nd ed.) SGE Editoriali Padova. 8886281757.

Lazzarin, R., & Crose, D. (2000). *Il soffitto radiante nella climatizzazione ambientale* (1st ed.). SGE Padova. 8886281498.

Lazzarin, R., & Noro, M. (2020). Energy analysis based on dynamic simulation of industrial heating by radiant modules with condensing unit. *AiCarr Journal*, *62*(3), 25–29.

Min, T. C., Schutrum, L. F., Parmelee, G. V., & Vouris, J. D. (1956). Natural convection and radiation in a panel heated room. *ASHRAE Transactions*, *62*, 337–358.

Noro, M., Mancin, S., & Cerboni, F. (2022a). High efficiency hybrid radiant and heat pump heating plants for industrial buildings: An energy analysis. *International Journal of Heat and Technology*, *40*(4), 863–870. https://doi.org/10.18280/ijht.400401

Noro, M., Mancin, S., & Cerboni, F. (2022b). Improving efficiency and renewables utilization by hybrid heating plants

for industrial buildings. 2022 IOP Conf. *IOP Conference Series: Earth and Environmental Science*, *1106*(1), 012013. https://doi.org/10.1088/1755-1315/1106/1/012013

Novoselac, A., Burley, B. J., & Srebric, J. (2006). *New convection, correlations for cooled ceiling panels in room with mixed and stratified airflow* (Vol. 122). HVAC&R Research. https://doi.org/10.1080/10789669.2006.10391179

Officine Termotecniche Fraccaro. Waterstrip (Termostrisce radianti), agg. 04/2017

Richter, B. K., Marcondes, G. H., Monteiro, N. J., da Costa, S. E. G., Loures, E. R., Deschamps, F., & de Lima, E. P. (2023). Industrial energy efficiency assessment and prioritization model: An approach based on multi-criteria method PROMETHEE. *International Journal of Sustainable Energy Planning and Management*, *37*, 41–60. https://doi.org/10.54337/ijsepm.7335

Schutrum, L. F., & Vouris, J. D. (1954). Effects of room size and non-uniformity of panel temperature on panel performance. *ASHRAE Transactions*, *60*, 1516.

Shook, P., Choi, J.-K., & Kissock, K. (2023). Analyzing the multiscale impacts of implementing energy-efficient HVAC improvements through energy audits and economic input-output analysis. *Journal of Energy Resources Technology, Transactions of the ASME*, *145*(4), 041701. https://doi.org/10.1115/1.4056116

Spiga, M. (2018). *Efficienza energetica e termofisica dell'edificio* (1st ed.). Società Editrice Esculapio - Bologna. 9788893850759.

Trianni, A., Cagno, E., & De Donatis, A. (2014). A framework to characterize energy efficiency measures. *Applied Energy*, *118*, 207–220. https://doi.org/10.1016/j.apenergy.2013.12.042

Vogt, M., Buchholz, C., Thiede, S., & Herrmann, C. (2022). Energy efficiency of Heating, Ventilation and Air Conditioning systems in production environments through model-predictive control schemes: The case of battery production. *Journal of Cleaner Production*, *350*, 131354. https://doi.org/10.1016/j.jclepro.2022.131354